



Cite this: *RSC Adv.*, 2022, 12, 26575

Received 29th July 2022  
Accepted 6th September 2022

DOI: 10.1039/d2ra04757h

rsc.li/rsc-advances

# Diamond-rich crystalline nanosheets seeded with a Langmuir monolayer of arachidic acid on water

Toshihiko Tanaka,<sup>a,†</sup> Yasuhiro F. Miura,<sup>†\*b</sup> Tetsuya Aoyama,<sup>cd</sup>  
Kazunori Miyamoto,<sup>e</sup> Yoshiya Akagi,<sup>b</sup> Masanobu Uchiyama<sup>ce</sup> and Eiji Osawa<sup>f</sup>

The enigmatic self-assembling ability of nanodiamond (ND) particles has been discovered herein. Diamond-rich crystalline nanosheets with thickness of approximately ~25 nm were grown from a Langmuir monolayer of arachidic acid (AA) at the interface between air and a dilute aqueous ND solution. Their fine rectangular shapes with uniform uniaxial birefringence indicate appreciable crystallinity, thus supporting that they are hydrated colloidal crystals of homogeneous ND particles.

## Introduction

Nanodiamond (ND) particles have attracted growing attention due to their promising potential applications,<sup>1–4</sup> and their self-assembly<sup>5–10</sup> from aqueous colloidal solutions is enigmatic because of the anisotropic precipitates produced. One of the authors (E. O.) reported the preparation of ND whiskers<sup>5</sup> through the slow drying of his commercialized solution, NanoAmando®, and Huang *et al.*<sup>6</sup> prepared fine microfibers from solutions of acid-treated ND particles. Petit *et al.* also reported an interesting cubic aggregate (1.7 × 1.7 mm; 0.8 mm thick) prepared from a colloidal solution of plasma-hydrogenated ND with HCl.<sup>8</sup> Why are these materials so anisotropic? Why are the aggregates rectangular?

We presume that the precipitates consist of similar ND particles in terms of both size and shape and that the particles can form a periodic crystal-like structure. If the particles differed in size and shape, the precipitates would not form, regardless of whether they were n-diamonds<sup>7</sup> or doped diamonds.<sup>8</sup> The concept of homogeneous ND particles was first predicted from DFT calculations<sup>11</sup> and we call them elementary diamond nanoparticles (EDIANS). The precipitates also appear to consist of similar EDIANS, however so far it has not been

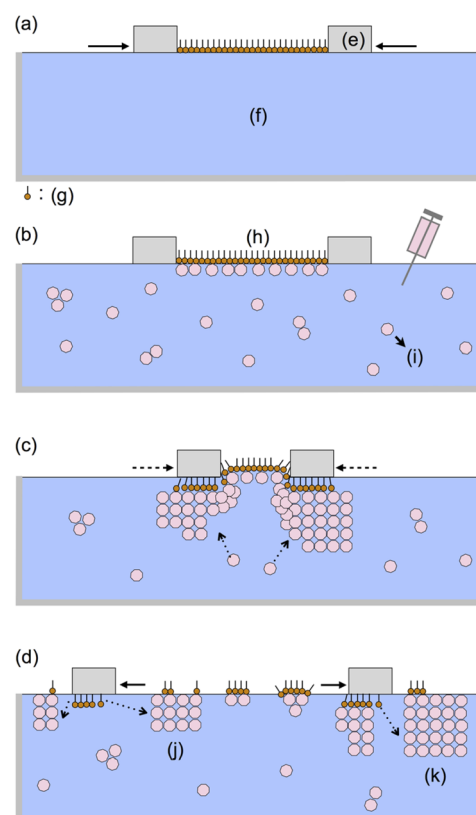


**Fig. 1** Preparation of nanosheets and a plausible model: (a) a Langmuir monolayer of AA (g) on water (f) between two PTFE bars (e); (b) injection of EDIANS (i) and a resulting AA monolayer with adsorbed ND (h); (c) a decrease in the area of the monolayer and plausible crystallization of ND particles along the soaked fringe of the PTFE bars; (d) nanosheets (j) or (k) generated on the water surface between or outside the bars when they are pulled apart.

<sup>a</sup>Chemistry and Biochemistry, Fukushima College, National Institute of Technology, 30 Azanagao, Tairakamiarakawa, Iwaki 970-8034, Fukushima, Japan. E-mail: 3116566701@jcom.home.ne.jp

<sup>b</sup>Hamamatsu University School of Medicine, 1-20-1 Handayama, Higashi-ku, Hamamatsu 431-3192, Shizuoka, Japan

<sup>c</sup>Elements Chemistry Laboratory, RIKEN Cluster for Pioneering Research (CPR), 2-1 Hirosawa, Wako 351-0198, Saitama, Japan

<sup>d</sup>Ultrahigh Precision Optics Technology Team, RIKEN Center for Advanced Photonics (RAP), 2-1 Hirosawa, Wako 351-0198, Saitama, Japan

<sup>e</sup>Graduate School of Pharmaceutical Sciences, The University of Tokyo, 7-3-1 Hongo, Bunkyo-ku 113-0033, Tokyo, Japan

<sup>f</sup>Nano Carbon Research Institute Ltd, Asama Research Extension Centre, Shinshu University, 3-15-1 Tokita, Ueda 386-8567, Nagano, Japan

<sup>†</sup> These authors contributed equally.



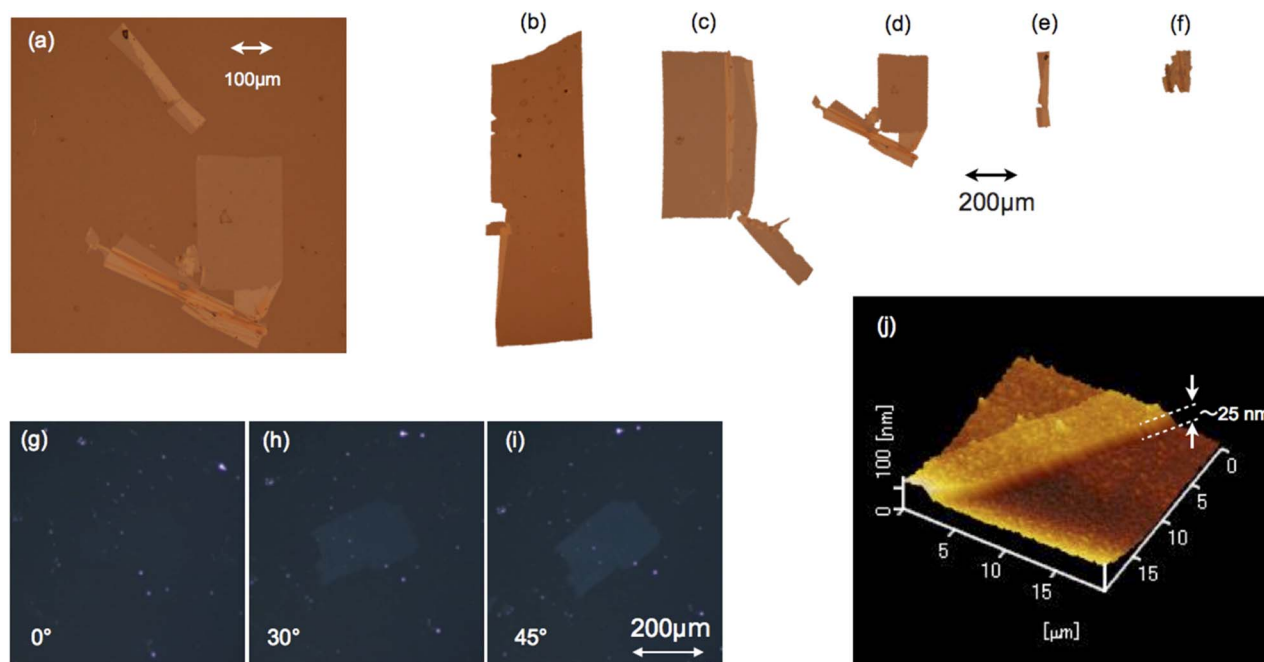


**Fig. 2** Microscopic images of nanosheets: (a) a reflective image; (b–f) trimmed reflective images; (g–i) transmission images of a nanosheet under crossed Nicols; (j) a 3D AFM image in tapping mode. The images (b–f) were obtained from the original images by erasing the background with PowerPoint (Microsoft, Inc.). The two polarization directions are vertical and horizontal in (g–i) and the in-plane sample rotation was 30° (h) or 45° (i) with respect to (g).

possible to isolate them and to determine their detailed structure experimentally.

Here we demonstrate the preparation of rectangular crystalline nanosheets (~25 nm thick) of ND from a monolayer of arachidic acid (AA:  $C_{19}H_{39}COOH$ ) at the interface between air and a dilute ND solution. Such crystalline ND nanosheets have not come to our knowledge and their anisotropy suggests that they consist of EDIANS containing ordered water molecules. Alternating layers of ND and polyelectrolyte were reported, being neither rectangular nor crystalline.<sup>9</sup>

## Experimental

The general procedure for nanosheet formation was as follows. AA (>99%) was purchased from Fluka AG (St. Gallen, Switzerland) and was used as received without further purification. Ultrapure water (18 MΩ cm) was obtained using a filter system (Direct-Q UV 3 Remote, Merck Millipore) to remove ions, organic matter, and small particles, and was used for all experiments and all cleaning steps. Chloroform (spectrophotometric grade) was purchased from Dojin Chemicals.

First, we prepared a Langmuir monolayer of AA on the water surface with a commercially available Langmuir–Blodgett trough (model 622, NIMA Instruments Ltd; area:  $68.4 \times 20 \text{ cm}^2$ ) at 25 °C by moving together two polytetrafluoroethylene bars ( $21.2 \times 1.6 \times 0.6 \text{ cm}^3$ ) as shown in Fig. 1a. The surface pressure was measured using a Wilhelmy-type balance. AA was spread on the water from a  $10^{-3} \text{ M}$  chloroform solution. After 5 min of air-drying, floating AA molecules were compressed to a surface pressure  $P$  of  $35 \text{ mN m}^{-1}$  at a rate of  $0.73 \text{ cm}^2 \text{ s}^{-1}$ . The area per

AA molecule  $S_A$  was  $0.23 \text{ nm}^2$  immediately after compression, which is close to the reported value.<sup>13</sup> Then, a dilute aqueous solution of ND (0.25 wt%, NanoAmando® Nanocarbon Research Institute, Inc.; diameter: 3.6 nm at 2.5 wt% by dynamic light scattering;  $\zeta$ -potential: 61 mV) was injected into the subphase (1500 mL water), further diluting the ND to 0.005 wt% (Fig. 1b).

After the injection of ND (Fig. 1c), the  $S_A$  value decreased remarkably while keeping the  $P$  value at  $35 \text{ mN m}^{-1}$  using the computer-controlled barriers; the compressed area  $S_A$  decreased by 46% for 0.5 h. The computer-controlled surface pressure was then decreased to  $10 \text{ mN m}^{-1}$ , and the further decrease in  $S_A$  was modest: 10% in 16.7 h. Up to this point, no sheets were observed at any position in the trough. However, immediately after pulling the bars apart, we observed innumerable ultrathin rectangular nanosheets (Fig. 1d).

For microscopic measurements including polarized microscopy, atomic force microscopy (AFM) and microscopic Raman spectra, the nanosheets were transferred on glass or silicon substrates as follows. Prior to the formation of the nanosheets at the air/water interface, the substrates were immersed in the subphase and placed on the bottom of the trough. After the growth, the floating nanosheets were transferred on the substrates located at the bottom of the trough by natural lowering of the air/water interface, which takes a few days through air-dry. The sheets were so fragile that we avoided mechanical shocks in the slow transfer process.

Samples for Raman spectra were deposited on silicon substrates and the spectra were recorded with a Raman



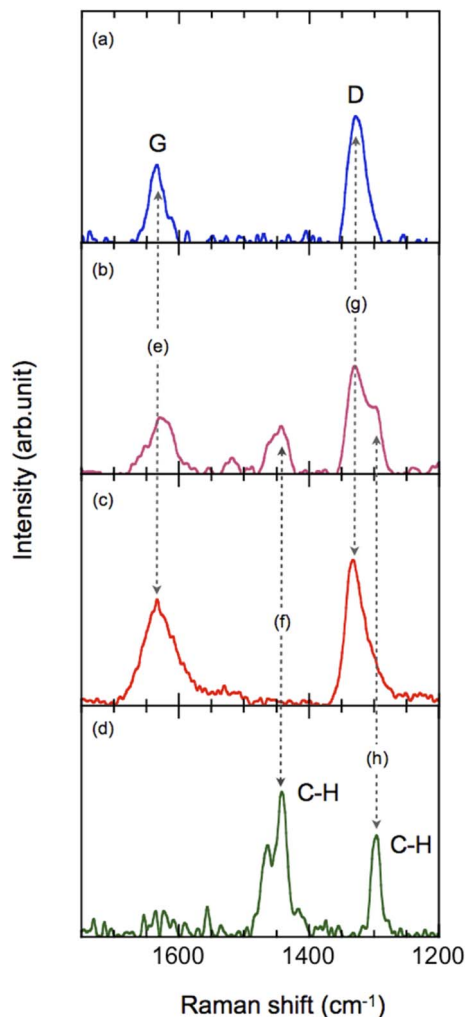


Fig. 3 Raman spectra of (a) a typical rectangular nanosheet; (b) the AA monolayer with adsorbed ND; (c) an air-dried drop of ND colloidal solution; and (d) an air-dried drop of AA solution. (e) The G-band is located at  $1630\text{--}1634\text{ cm}^{-1}$ . (f) A C–H stretching mode is located at  $1442\text{ cm}^{-1}$ . (g) D-band at  $1330\text{--}1332\text{ cm}^{-1}$ . (h) A C–H bending mode is located at  $1296\text{ cm}^{-1}$ .

spectrometer (NRS-4500, JASCO) equipped with a microscope. The excitation beam (16.1 mW) focused on a spot of nearly  $2\text{ }\mu\text{m}$  on each sample. The AA monolayer with ND (Fig. 1b) was also transferred onto a hexamethyldisilazane-modified silicon substrate utilizing horizontal lifting method (Langmuir–Schaefer method).<sup>14</sup> For reference spectra, an air-dried drop of the ND aqueous colloidal solution (2.5 wt%) or that of AA the chloroform solution ( $10^{-3}\text{ M}$ ) was prepared on the substrates.

## Results and discussion

Most of the nanosheets were rectangular and their long sides typically ranged from approximately  $0.2$  to  $10\text{ }\mu\text{m}$  as shown by micrographs of typical deposited sheets in Fig. 2a–f. Their shapes were clear in reflective images, and we found many

sheets of various sizes. They were frequently folded or torn by unavoidable water flows while a part of the nanosheets was in contact with the substrate during deposition, creating defects such as voids and folds (Fig. 2a–f). These results indicate that the nanosheets had fine rectangular shapes on the water. Their typical thickness was  $25\text{ nm}$  as observed by AFM (NanoNavi IIS/NanoCute, Seiko Instruments Inc.) in dynamic force mode (Fig. 2j).

Each nanosheet was uniformly birefringent, indicating crystallinity with uniaxial optical anisotropy. Under crossed-Nicols of a polarizing microscope (Eclipse E600 POL, Nikon), a nanosheet was darkest with the long side parallel to one of the two polarization directions and became brightest at when the long side was rotated laterally  $45^\circ$  with respect to these two directions (Fig. 2g–i). Because of the small thickness of the nanosheets, the brightness was too low to show clear contrast in printed materials; nevertheless, the contrast was clearly seen through careful observations.

ND particles are highly hygroscopic<sup>5</sup> and the nanosheets on the water contain significant amount of water at the air–water interface. Hence, the EDIAs should organize into a kind of hydrated colloidal crystal there.

Raman spectra showed that, after injection, the ND particles adsorbed onto the AA monolayer. The deposited monolayer (Fig. 3b) showed the D and G bands<sup>15–21</sup> of ND (Fig. 3e and g) together with the CH stretching mode of AA (Fig. 3f and h).

The rectangular nanosheets consist of ND particles. The D and G bands of ND were observed whereas the CH stretching mode of AA was not observed (Fig. 3a). The thickness of  $25\text{ nm}$  indicates that the nanosheets contain at least 4–7 layers of EDIAs. Presumably the crystals also contain tiny amounts of AA molecules because they formed from ND adsorbed on the AA monolayer, but we consider that most parts of the nanosheets were not covered with AA as illustrated in Fig. 1k. Hence, they are diamond-rich nanosheets.

The Raman spectra of ND (Fig. 3a–c) were successfully obtained using the fluorescence subtraction method with a laser ( $532\text{ nm}$ ) as the excitation source. The ND particles having a diameter of less than  $4\text{ nm}$  possibly contributed this success. The fluorescence should decrease with decreasing ND particle size because of the significant structural deformation recently confirmed by high-resolution transmission electron microscopy (TEM)<sup>22</sup> and should affect nitrogen-vacancy centers.<sup>23–27</sup>

Most of the nanosheets were found near the PTFE bars and thus crystallization of ND took place during or after the decrease in  $S_A$  upon contact with the PTFE bars, thus yielding the nanosheets along the soaked fringe of the bars (Fig. 1d). Without AA molecules, a dilute ND solution ( $0.005\text{ wt}\%$ ) never generated any sheets at the air–water interface. Hence, the nanosheets are seeded by the AA monolayer. Polyanionic nanosheets of  $[(\text{Ca}_2\text{Nb}_3\text{O}_{10})^-]_n$  (CNO) can be obtained from dilute colloidal suspensions of CNO in a similar process involving crystallization of CNO after adsorption to a  $[\text{N}(\text{CH}_3)_2(\text{C}_{18}\text{H}_{37})_2]$  (DOA) monolayer.<sup>28</sup> There should be Coulombic attractive forces in both of these cases: between CNO anions and DOA cations and between AA<sup>−</sup>



(C<sub>19</sub>H<sub>39</sub>COO<sup>−</sup>) and positively charged ND particles, as indicated by the positive  $\zeta$ -potential of NanoAmand®. Most of the AA molecules should be dissociated in the subphase (pH  $\approx$  6).

The details of this self-organized structure remain an enigmatic open question. In excellent TEM images,<sup>22</sup> ND particles are usually so different that they cannot form crystals. Why are they crystallized?

We do not presume that the ND particles in the nanosheets are as different as those in the images. It should be noted that homogeneous EDIANS are likely to be purified through crystallization. If NanoAmand® contains the EDIANS appreciably, they may be crystallized. Another consideration must be the possible deformation due to the electron beam. Although the use of a low voltage (80 keV) with aberration correction successfully minimized the deformation,<sup>22</sup> we can not exclude its possibility entirely.

After hydrated colloidal crystals are deposited on solid substrates, their crystalline order is expected to be decreased significantly by drying. After losing water molecules, the hydrated colloidal crystals must be broken. Small grains can be seen on their surface in Fig. 2j and therefore were formed by aggregation during drying. Perhaps the crystals do not lose all their water molecules and keep some of them depending on ambient humidity and/or temperature. Heat treatment will also remove water molecules from the nanosheets and the focused laser light may cause such heating in the Raman measurements. It should be noted therefore that we measured the nanosheets after such drying.

The potentially organized structure of the ND nanosheets and their small thickness also suggest various applications, particularly on surfaces, as lubricants,<sup>29–31</sup> catalysts<sup>32–36</sup> chemical vapor deposition seeds,<sup>37–39</sup> and drug delivery films.<sup>12,40–43</sup> In these applications, does the organized structure have any effect? That will be fascinating.

## Conclusions

Rectangular crystalline nanosheets ( $\sim$ 25 nm thick) of ND can be prepared from an AA monolayer on a water subphase containing ND particles in the following two steps: (1) adsorb ND particles onto the AA monolayer and (2) crystallize the ND particles by compressing the AA monolayer horizontally. The nanosheets are hydrated colloidal crystals of ND particles.

We believe that the nanosheets are the hydrated colloidal crystals of homogeneous EDIANS. Otherwise, there is not a plausible explanation for their rectangular shapes, ultra thin thickness, and uniform birefringence. To determine their crystal structure, further analysis under wet conditions is expected and we are now proceeding with *in situ* X-ray diffraction measurements<sup>44</sup> of the ND nanosheets on water. The hydrated colloidal crystals on water may keep their water molecules. However, the crystals move easily and are hardly fixed for the measurements. Although a long time will be required to complete the measurements, it could be the rediscovery of ND as a novel chemical species.

## Author contributions

Toshihiko Tanaka: writing-original draft, methodology, nanosheet formation, conceptualization and supervision; Yasuhiro F. Miura: methodology, nanosheet formation, conceptualization and supervision; Tetsuya Aoyama: microscopic analysis; Kazunori Miyamoto: Raman Analysis; Masanobu Uchiyama: Raman analysis; Yoshia Akagi: nanosheet formation; and Eiji Osawa: ND solutions.

## Conflicts of interest

There are no conflicts to declare.

## Acknowledgements

We would like to acknowledge the following five students of Fukushima College for their excellent contribution on the engineering for Langmuir films: Mr Masamichi Hoshi, Mr Hyuga Kaneko, Mr Takumi Sato, Mr Nagito Haga, and Mr Daiki Ayai. This work was partly supported by JSPS KAKENHI grant number JP21K04813.

## References

- 1 E. Osawa, *et al.*, *Nanodiamonds: Applications in Biology and Nanoscale Medicine*, ed. D. Ho, Springer Science+Business Media, Inc., Norwell, MA, 2010.
- 2 A. Vul', *et al.*, *Detonation Nanodiamonds: Science and Applications*, ed. Alexander Vul' and Olga Shenderova, CRC Press, FL, 2013.
- 3 A. S. Barnard, *et al.*, *Nanodiamond, RSC Nanoscience & Technology Book No. 31*, ed. Oliver A Williams, The Royal Society of Chemistry, London, 2014.
- 4 C. E. Nebel, *et al.*, *Nanodiamonds: Advanced Material Analysis, Properties and Applications*, ed. Jean-Charles Arnault, Elsevier, 2017.
- 5 E. Osawa, *Diamond Relat. Mater.*, 2007, **16**, 2018.
- 6 H. Huang, L. Dai, D. H. Wang, L.-S. Tanc and E. Osawa, *J. Mater. Chem.*, 2008, **18**, 1347.
- 7 M. L. Terranova, D. Manno, M. Rossi, A. Serra, E. Filippo, S. Orlanducci and E. Tamburri, *Cryst. Growth Des.*, 2009, **9**, 1245–1249.
- 8 T. Petit, H. A. Girard, A. Trouvé, I. Batonneau-Gener, P. Bergonzola and J.-C. Arnault, *Nanoscale*, 2013, **5**, 8958.
- 9 T. Yoshikawa, V. Zuerbig, F. Gao, R. Hoffmann, C. E. Nebel, O. Ambacher and V. Lebedev, *Langmuir*, 2015, **31**, 5319.
- 10 S. S. Batsanov, D. L. Guriev, S. M. Gavrilkin, K. A. Hamilton, K. Lindsey, B. G. Mendis, H. J. Riggs and A. S. Batsanov, *Mater. Chem. Phys.*, 2016, **173**, 325.
- 11 A. S. Barnard, *J. Mater. Chem.*, 2008, **18**, 4038.
- 12 H. Huang, E. Pierstorff, Eiji Osawa and D. Ho, *ACS Nano*, 2008, **2**, 203.
- 13 M. A. Valdes-Covarrubias, R. D. Cadena-Nara, E. Vásquez-Martínez, D. Valdez-Péres and J. Ruiz-García, *J. Phys.: Condens. Matter*, 2004, **16**, S2097.





- 14 A. Ulman, *An Introduction to Ultrathin Organic Films: from Langmuir-Blodgett to Self-Assembly*, Academic Press, San Diego, CA, 1991, p. 127.
- 15 A. C. Ferrari and J. Robertson, *Philos. Trans. R. Soc. London, Ser. A*, 2004, **362**, 2477.
- 16 B. V. Spitsyn, L. Davidson, M. N. Gradoboev, T. B. Galushko, N. V. Serebryakov, T. A. Karpukhina, I. I. Kulakovac and N. N. Melnik, *Diamond Relat. Mater.*, 2006, **15**, 296.
- 17 V. Mochalin, S. Osswald and Y. Gogotsi, *Chem. Mater.*, 2009, **21**, 273.
- 18 S. Osswald, V. N. Mochalin, M. Havel, G. Yushin and Y. Gogotsi, *Phys. Rev. B*, 2009, **80**, 075419.
- 19 V. I. Korepanov, H. Witek, H. Okajima, E. Osawa and H. Hamaguchi, *J. Chem. Phys.*, 2014, **140**, 041107.
- 20 M. Popov, V. Churkin, A. Kirichenko, V. Denisov, D. Ovsyannikov, B. Kulnitskiy, I. Perezhogin, V. Aksenenkov and V. Blank, *Nanoscale Res. Lett.*, 2017, **12**, 561, 1.
- 21 M. Mermoux, L.-Y. Chang, H. A. Girard and J.-C. Arnault, *Diamond Relat. Mater.*, 2018, **87**, 248.
- 22 S. L. Y. Chang, C. Dwyer, E. Osawa and A. S. Barnard, *Nanoscale Horiz.*, 2018, **3**, 213.
- 23 A. Gruber, A. Drabenstedt, C. Tietz, L. Fleury, J. Wrachtrup and C. von Borczyskowski, *Science*, 1997, **276**, 1202.
- 24 M. W. Doherty, N. B. Manson, P. Delaney, F. Jelezko, J. Wrachtrup and L. C. L. Hollenberg, *Phys. Rep.*, 2013, **528**, 1.
- 25 S.-J. Yu, M.-W. Kang, H.-C. Chang, K.-M. Chen and Y.-C. Yu, *J. Am. Chem. Soc.*, 2005, **127**, 17604.
- 26 R. Igarashi, Y. Yoshinari, H. Yokota, T. Sugi, F. Sugihara, K. Ikeda, H. Sumiya, S. Tsuji, I. Mori, H. Tochio, Y. Harada and M. Shirakawa, *Nano Lett.*, 2012, **12**, 5726.
- 27 S. Sotoma, D. Terada, T. F. Segawa, R. Igarashi, Y. Harada and M. Shirakawa, *Sci. Rep.*, 2018, **8**, 5463.
- 28 K. Ikegami, H. Tetsuka, Y. Hoshi, T. Ebina and H. Takashima, *Langmuir*, 2010, **26**, 2514.
- 29 J.-Y. Lee and D.-S. Lim, *Surf. Coat. Technol.*, 2004, **188–189**, 534.
- 30 A. V. Sumant, D. S. Grierson, J. E. Gerbi 2, J. A. Carlisle, O. Auciello and R. W. Carpick, *Phys. Rev. B*, 2007, **76**, 235429.
- 31 O. Elomaa, T. J. Hakala, V. Myllymäki, J. Oksanen, H. Ronkainen, V. K. Singh and J. Koskinen, *Diamond Relat. Mater.*, 2013, **34**, 89.
- 32 W. W. Zheng, Y. H. Hsieh, Y. C. Chiu, S. J. Cai, C. L. Cheng and C. Chen, *J. Mat. Chem.*, 2009, **19**, 8432.
- 33 J. Zhang, D. S. Su, R. Blume, R. Schlog, R. Wang, X. Yang and A. Gajovic, *Angew. Chem., Int. Ed.*, 2010, **49**, 8640.
- 34 Y. Liu, S. Chen, X. Quan, H. Yu, H. Zhao, Y. Zhang and G. Chen, *J. Phys. Chem. C*, 2013, **117**, 14992.
- 35 A. Ahmed, S. Mandal, L. Gines, O. A. Williams and C.-L. Cheng, *Carbon*, 2016, **110**, 438.
- 36 Y. Ding, X. Huang, X. Yi, Y. Qiao, X. Sun, A. Zheng and D. S. Su, *Angew. Chem., Int. Ed.*, 2018, **57**, 13800.
- 37 O. A. Williams, O. Douhéret, M. Daenen, K. Haenen, E. Osawa and M. Takahashi, *Chem. Phys. Lett.*, 2007, **445**, 255.
- 38 N. Yang, H. Uetsuka, E. Osawa and C. E. Nebel, *Nano Lett.*, 2008, **8**, 3572.
- 39 E. L. H. Thomas, S. Mandal, A. Ahmed, J. E. Macdonald, T. G. Dane, J. Rawle, C.-L. Cheng and O. A. Williams, *ACS Omega*, 2017, **2**, 6715.
- 40 H. Huang, E. Pierstorff, E. Osawa and D. Ho, *Nano Lett.*, 2007, **7**, 3305.
- 41 R. Lam, M. Chen, E. Pierstorff, H. Huang, E. Osawa and D. Ho, *ACS Nano*, 2008, **2**, 2095.
- 42 H. Huang, M. Chen, P. Bruno, R. Lam, E. Robinson, D. Gruen and D. Ho, *J. Phys. Chem. B*, 2009, **113**, 2967.
- 43 X. Li, J. Shao, Y. Qin, C. Shao, T. Zheng and L. Ye, *J. Mater. Chem.*, 2011, **21**, 7966.
- 44 K. Kjaer, J. Als-Nielsen, C. A. Helm, P. Tippman-Krayer and H. Möhwald, *J. Phys. Chem.*, 1989, **93**, 3200.

